Article

Exciton–Plasmon Interaction in a Composite Metal–Insulator–Semiconductor Nanowire System

Yuri Fedutik, Vasily Temnov, Ulrike Woggon, Elena Ustinovich, and Mikhail Artemyev

J. Am. Chem. Soc., **2007**, 129 (48), 14939-14945 • DOI: 10.1021/ja074705d

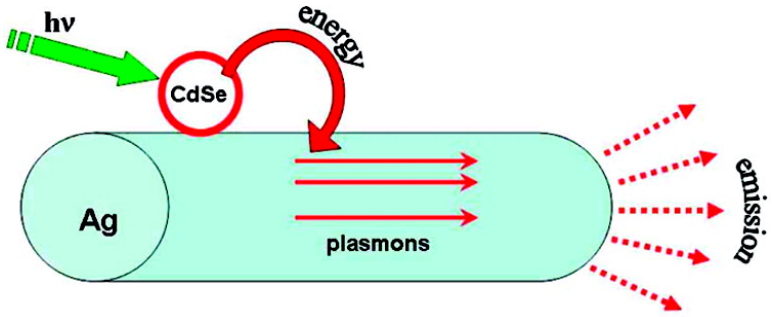

More About This Article

Additional resources and features associated with this article are available within the HTML version:

- Supporting Information
- Access to high resolution figures
- Links to articles and content related to this article
- Copyright permission to reproduce figures and/or text from this article

View the Full Text HTML

J|A|C|S
ARTICLES
Published on Web 11/10/2007

Exciton−Plasmon Interaction in a Composite Metal−Insulator−Semiconductor Nanowire System

Yuri Fedutik,[†] Vasily Temnov,[†] Ulrike Woggon,[†] Elena Ustinovich,[‡] and Mikhail Artemyev*[,‡]

Contribution from Fachbereich Physik, Universität Dortmund, Otto-Hahn-Str. 4, 44227, Dortmund, Germany, and Institute for Physico-Chemical Problems of Belarussian State University, Leningradskaya Str., 14, Minsk 220080, Belarus

Received June 27, 2007; E-mail: mikhail.artemyev@bigfoot.com

Abstract: We report about the synthesis and optical properties of a composite metal−insulator−semiconductor nanowire system which consists of a wet-chemically grown silver wire core surrounded by a SiO_2 shell of controlled thickness, followed by an outer shell of highly luminescent CdSe nanocrystals. With microphotoluminescence (μ-PL) experiments, we studied the exciton−plasmon interaction in individual nanowires and analyzed the spatially resolved nanocrystal emission for different nanowire length, SiO_2-shell thickness, nanocrystal shape, pump power, and emission polarization. For an SiO_2 spacer thickness of ∼15 nm, we observed an efficient excitation of surface plasmons by excitonic emission of CdSe nanocrystals. For nanowire lengths up to ∼10 μm, the composite metal−insulator−semiconductor nanowires ((Ag)SiO_2)CdSe act as a waveguide for 1D-surface plasmons at optical frequencies with efficient photon outcoupling at the nanowire tips, which is promising for efficient exciton−plasmon−photon conversion and surface plasmon guiding on a submicron scale in the visible spectral range.

Introduction

The electromagnetic interaction of molecules with metallic surfaces has been an intensively studied research field for many years. Interest in this subject has been stimulated by manifold experimental evidence demonstrating that surface-enhanced Raman scattering and surface-enhanced fluorescence of molecules, ions, and quantum dots (QDs) were observed near metals with controlled surface roughness, such as gratings, metal islands, or particle arrays. Very recently, the properties of surface electromagnetic waves (surface plasmons, SP) on nanostructured metal-dielectric interfaces attracted a considerable scientific and technological interest and led to an explosive development in nanoplasmonics.[1] The recent experiments in nanoplasmonics demonstrated the propagation of SPs over macroscopic distances, the focusing of SPs by plasmonic lenses,[2] the effect of SP reflection with nearly 100% efficiency by SP Bragg mirrors,[3] suitable to build up SP interferometers,[4,5] and so forth. Although the majority of experimental investigations were performed on 2D-metal surfaces nanostructured by a focused ion beam (FIB), some of the studies dealt with chemically grown, high aspect ratio metallic nanowires, i.e., ∼100 nm in diameter and ∼10 μm in length, providing the additional functionality of 1D-guiding of SPs[6] or acting as plasmonic nanocavities.[7] All such devices rely on the direct excitation of SPs in metallic nanostructures by incident light beams.

Of special interest is the excitation of SPs by excited molecules and QDs, a much less studied issue in nanoplasmonics and particularly important for fundamental light−matter interaction phenomena.[8,9] These light-emitting nano-objects may serve not only as tiny localized dipole emitters, but also as receivers in an energy back-conversion from plasmons to excitons. The coupling of nanocrystal excitons with SPs in a composite metal−insulator−semiconductor nanowire system would allow for transformation of light absorbed (and re-emitted) by the semiconductor nanocrystals (NCs) into SPs and back to photons. Such composite nanostructures might be of great perspective as elements of future computer chips. The combination of plasmonic nanostructures and semiconductor NCs may be especially useful here, because of some advantageous properties of such nanocrystals, such as the following: (i) chemically synthesized CdSe, CdTe, CdS, ZnSe, and so forth, NCs exhibit very bright photoluminescence (PL) (chemi- and electroluminescence as well), with quantum yields exceeding 50% at room temperature; (ii) the emission wavelength can be precisely tuned over a very wide spectral range (∼300−3000

[†] Universität Dortmund.
[‡] Belarussian State University.

(1) Barnes, W. L.; Dereux, A.; Ebbesen, T. W. *Nature* **2003**, *424*, 824−830.
(2) Yin, L.; Vlasko-Vlasov, V. K.; Pearson, J.; Hiller, J. M.; Hua, J.; Welp, U.; Brown, D. E.; Kimball, C. W. *Nano Lett.* **2005**, *5*, 1399−1402.
(3) Gonzalez, M. U.; Weeber, J.-C.; Baudrion, A.-L.; Dereux, A.; Stepanov, A. L.; Krenn, J. R.; Devaux, E.; Ebbesen, T. W. *Phys. Rev. B* **2006**, *73*, 155416−1 to 155416−13.
(4) Bozhevolnyi, S. I.; Volkov, S. V.; Devaux, E.; Laluet, J.; Ebbesen, T. W. *Nature* **2006**, *440*, 508−511.
(5) Temnov, V. V.; Woggon, U.; Dintinger, J.; Devaux, E.; Ebbesen, T. W. *Opt. Lett.* **2007**, *32*, 1235−1237.
(6) Dickson, R. M.; Lyon, L. A. *J. Phys. Chem. B* **2000**, *104*, 6095−6098.
(7) Ditlbacher, H.; Hohenau, A.; Wegener, D.; Kreibig, U.; Rogers, M.; Hofer, F.; Aussenegg, F. R.; Krenn, J. R. *Phys. Rev. Lett.* **2005**, *95*, 257403−1 − 257403−4.
(8) Temnov, V. V.; Woggon, U. *Phys. Rev. Lett.* **2005**, *95*, 243602−1 to 243602−4.
(9) Chang, D. E.; Sørensen, A. S.; Hemmer, P. R.; Lukin, M. D. *Phys. Rev. Lett.* **2006**, *97*, 053002−1 to 053002−1.

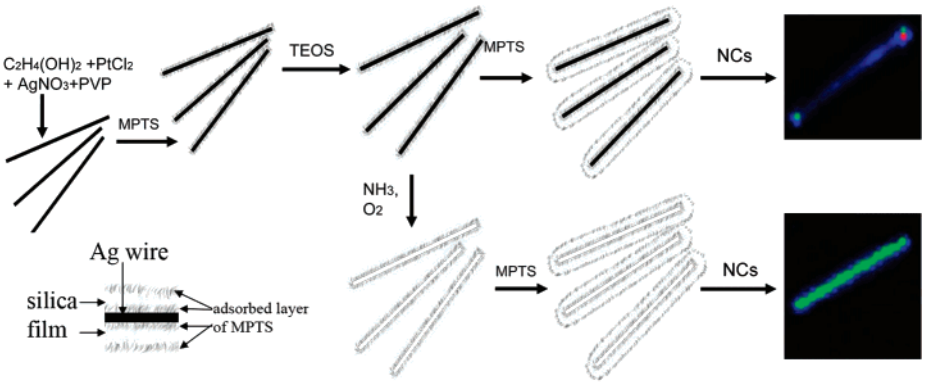

Figure 1. Preparation of composite (Ag)SiO_2 and hollow SiO_2 nanowires capped with highly luminescent CdSe NCs. The first steps consist of the synthesis of silver nanowires via the polyol process (upper left) followed by the activation of the silver surface with MPTS. Next, the SiO_2 shell is formed on the activated silver surface by the hydrolysis of TEOS. Hollow SiO_2 nanowire can be prepared on this stage by selective etching of the silver core in ammonia. In the last step, both Ag/SiO_2− and hollow SiO_2 nanowires were covered with CdSe NCs by subsequent activation of the SiO_2 surface with MPTS followed with NCs deposition from their colloidal solution via MPTS−NC bond formation.

nm) by changing the size or composition of the NCs; (iii) contrary to organic molecules and rare-earth and other ions, semiconductor NCs can be optically excited in a very broad spectral range; and (iv) the stability of semiconductor NCs against photodegradation is three orders of magnitude greater than that of widely known organic luminophores.[10−12] Recently, semiconductor NCs have already been coupled to different metallic structures (thin films, colloidal nanoparticles, metallic shells) to tailor optical emission of QD-excitons.[13−15]

In this work, we focus on the utilization of exciton−plasmon interactions in silver nanowires to obtain 1D-waveguiding on micrometer length scales. ((Ag)SiO_2)NCs, a composite metal−insulator−semiconductor nanowire system, has been synthesized with wet-chemically grown silver nanowire core surrounded by a SiO_2 shell of controlled thickness, followed by an outer shell of highly luminescent CdSe NCs. A systematic study of the spatially and spectrally resolved nanocrystal emission is carried out for different SiO_2 shell thicknesses, nanowire lengths, and CdSe NC shape, i.e., spherical quantum dots (QDs) and elongated cylindrical nanorods (NRs). As a result, we demonstrate efficient exciton−plasmon coupling, SP-assisted waveguiding with efficient photon outcoupling at the nanowire tips for SiO_2 spacer thicknesses in the range of $d \approx 15$ nm and nanowire lengths up to $L \approx 10$ μm.

Experimental Section

Chemicals and Materials. Ethylene glycol (EG, 99.8%), platinum (II) chloride (99.99%), silver nitrate (99%), poly (vinyl pyrrolidone) (PVP, MW 40 000), 3-mercaptopropyltrimethoxysilane (MPTS, 98%), tetraethylorthosilicate (TEOS), methanol, 2-propanol, trichloroethylene, and toluene were purchased from Aldrich. EG was dehydrated by heating at 160 °C within 3 h. All other chemicals were used without further purification.

Preparation of Samples. Highly luminescent (CdSe)ZnS core−shell QDs and NRs were synthesized via standard high-temperature reaction.[16,17] The NCs with diameters of about 3.5 nm show a PL band centered at 605 nm. Typical (CdSe)ZnS NRs have a core diameter of 4 nm and a length of 25 nm. Before use, QDs and NRs were purified by precipitation with methanol from their colloidal solution in trichloroethylene, followed by dissolution in fresh portion of trichloroethylene.

Preparation of Silver Nanowires. Silver nanowires were prepared by modified polyol method.[18] Platinum nanoparticles of ~5 nm diameter serving as seeds for Ag-nanowire growth were synthesized by reducing $PtCl_2$ dissolved in EG. Then, a EG solution of PVP (50 mg/3 mL) containing silver nitrate (50 mg/3 mL) was added dropwise at a rate of approximately 0.1 mL/min to the stirred EG solution with platinum seeds at 160 °C. Temperature and stirring were kept constant for 60 min after completing reagents injection. Heterogeneous nucleation and growth of silver nanoparticles in the presence of PVP as a surface modifier resulted in the formation of uniform, almost monocrystalline silver nanowires. The resulting opaque gray-green solution contains silver nanowires and spherical nanoparticles which can be separated using size separation procedures.[19] Briefly, 5 mL of nanowire solution in EG was diluted with 45 mL of acetone and centrifuged at 2000 rpm for 15 min. The liquid phase containing mostly small spherical nanoparticles was removed, and the nanowires were redispersed in a fresh portion (5 mL) of EG. This procedure was repeated two times to achieve better separation of nanowires. The as-grown Ag-nanowires have a diameter of approximately 150 nm and a length ranging from one to several tens of micrometers.

Growth of the SiO_2 Shell. To functionalize silver nanowires with luminescent CdSe NCs, a SiO_2 shell of controlled thickness d has been introduced as a spacer between the surface of the silver nanowires and the CdSe NCs. The presence of a controlled-thickness spacer is important for finding the optimum exciton−plasmon interaction length similar to those observed in experiments with enhanced plasmon-assisted luminescence.[7] Schematic illustration of the preparation procedure is presented in Figure 1. The coating of silver nanowires with an amorphous SiO_2 shell was carried out by the Stöber method, which has been widely used to create SiO_2 coatings on different nanoparticles.[20] In a typical procedure, the silver nanowires were separated from its original EG solution, washed out by water, acetone, and toluene and redispersed in 1% solution of MPTS in toluene. The suspension was kept under slow stirring for 1 h at room temperature. MPTS creates a monolayer atop the silver nanowires, thus activating

(10) Murray, C. B.; Kagan, C. R.; Bawendi, M. G. *Annu. Rev. Mater. Sci.* **2000**, *30*, 545−610.
(11) Bruchez, M., Jr.; Moronne, M.; Gin, P.; Weiss, S.; Alivisatos, A. P. *Science* **1998**, *281*, 20213−2016.
(12) Sukhanova, A.; Venteo, L.; Devy, J.; Artemyev, M.; Oleinikov, V.; Pluot, M.; Nabiev, I. *Lab. Invest.* **2002**, *82*, 1259−1261.
(13) Kulakovich, O.; Strekal, N.; Yaroshevich, A.; Maskevich, S.; Gaponenko, S.; Nabiev, I.; Woggon, U.; Artemyev, M. *Nano Lett.* **2002**, *2*, 1449−1452.
(14) Gryczynski, I.; Malicka, J.; Jiang, W.; Fischer, H.; Chan, W. C. W.; Gryczynski, Z.; Grudzinski, W.; Lakowicz, J. R. *J. Phys. Chem. B* **2005**, *109*, 1088−1093.
(15) Lee, J.; Govorov, A. O.; Dulka, J.; Kotov, N. A. *Nano Lett.* **2004**, *4*, 2323−2330.
(16) Qu, L.; Peng, X. *J. Am. Chem. Soc.* **2002**, *124*, 2049−2055.
(17) Mokari, T.; Banin, U. *Chem. Mater.* **2003**, *15*, 3955−3960.
(18) Sun, Y.; Xia, Y.; *J. Am. Chem. Soc.* **2004**, *126*, 3892−3901.
(19) Sun, Y.; Gates, B.; Mayers, B.; Xia, Y. *Nano Lett.* **2002**, *2*, 165−168.
(20) Stöber, W.; Fink, A.; Bohn, E. *J. Coll. Interface. Sci.* **1968**, *26*, 62−69.

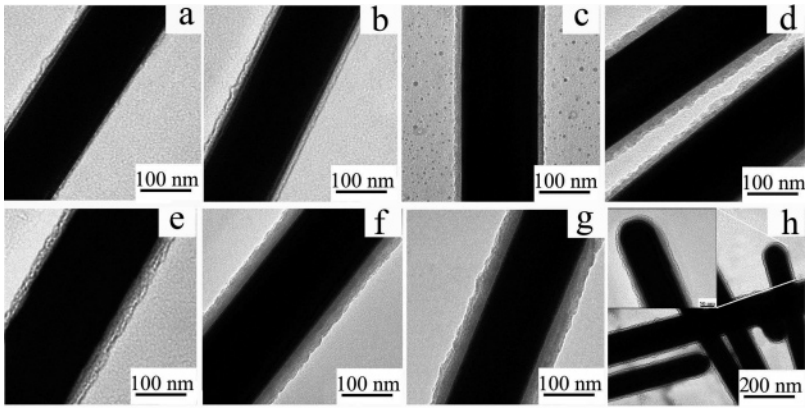

Figure 2. TEM images of silver nanowires covered with a SiO_2 shell of different thickness *d*. The d_{SiO_2} is controlled by the concentration of TEOS. The average thickness of SiO_2 shell increases from *a* to *g* (*a* ≈ 4 nm, *b* ≈ 13 nm, *c* ≈ 16 nm, *d* ≈ 22 nm, *e* ≈ 29 nm, *f* ≈ 32 nm, and *g* ≈ 38 nm). (h) TEM images of silver nanowire tips covered with SiO_2 demonstrate good homogeneity of the SiO_2 shell over the whole nanowire.

their surface to subsequent SiO_2 growth. The activated nanowires were washed with toluene, propanol, and redispersed in a mixture of propanol and water (4:1) to which 0.5 mL of 25% ammonia was added as the catalyst to speed up the hydrolysis of TEOS and SiO_2 deposition. The average thickness of the SiO_2 layer was determined by TEM measurements.

Approximately 25 μg of silver nanowires were redispersed in 25 mL of propanol−water−ammonia mixture to which the calculated amount of TEOS added under continuous stirring. After 1 h, a 2.5-mL aliquot of reaction mixture was centrifuged at 4000 rpm, the precipitate washed by 2-propanol, toluene, and redispersed in toluene. Simultaneously, the next portion of TEOS was added to the reaction mixture to continue the growth of the SiO_2 layer. These procedures were repeated several times, and a row of silver nanowires covered with different SiO_2 thicknesses *d* finally was obtained. Figure 2 shows TEM images of the silver nanowires covered with SiO_2 layer of controlled thickness. It is clearly seen that the SiO_2 layer covers homogeneously the silver nanowires including their tips (Figure 2h) with *d* varying from 4 nm in Figure 2a to 38 nm in Figure 2g. At this stage, hollow dielectric SiO_2 nanowires can be prepared by prolonged (24 h) selective etching of the silver core in ammonia (pH 10.5) in the presence of atmospheric oxygen.[21] After dissolution of the silver core, the reference samples without Ag-core were washed several times by water, propanol, and toluene and redispersed in toluene.

Attachment of CdSe Nanocrystals. Both (Ag)SiO_2 and hollow dielectric SiO_2 nanowires were covered with a submonolayer of highly luminescent CdSe QDs and NRs. First, the surface of SiO_2 layer was activated by MPTS on both types of composite nanowires. To accomplish this, the samples were dispersed in 1% solution of MPTS in toluene and kept at room temperature for 24 h in the inert atmosphere. Then, the samples were washed several times with toluene and redispersed in trichloroethylene, to which a colloidal solution of CdSe NCs in trichloroethylene was added. The mixture was stirred for 1 h, and the nanowires with NCs centrifuged and washed several times with trichloroethylene. The attachment of CdSe NCs to the SiO_2 surface was achieved by chemical interaction with free thiol groups of the MPTS monolayer.

The samples for TEM measurements were prepared by placing a small droplet of a suspension of composite nanowires on TEM copper grids and drying them at room temperature. TEM images were taken using a Gemini Leo microscope operated at 80 kV. For the optical measurements, a droplet of suspension was placed onto quartz glass and dried at room temperature in the dark.

Optical Experiments. The spatially and spectrally resolved PL of single composite nanowires was measured by imaging spectroscopy at the diffraction limit. The experimental micro-PL setup used in our experiments is shown in Figure 3. The samples were excited by a cw solid-state laser operating at $\lambda = 532$ nm with output power ranging from 0.1 mW to 5 W and a laser beam focused to a spot size of about 30 μm. The two excitation geometries with samples on a flat glass plate and on the prism (Kretschmann−Raether configuration) used in our experiments are illustrated in the panels of Figure 3. The emitted light was collected by a microscope objective (63×, NA = 0.95) and focused to a pinhole placed in the intermediate image plane (not shown in the sketch for the purpose of simplicity). Then the beam was again collimated, passed through a polarizer and a cutoff filter to remove the scattered laser light, and focused on a 256 × 1024 pixel chip of the cryogenically cooled Roper Scientific SPEC-10 CCD camera. The polarization vector of the linearly polarized excitation beam was controlled by rotating a half-wave plate and the polarization components of the emitted light were selected by rotating a polarizer in the emission beam path.

The configuration with flat glass plate (Figure 3a) was used for the experiments with different polarization of the incident laser beam. The measurements of the emission intensity versus SiO_2 shell thickness were performed within Kretschmann−Raether configuration. This configuration is suitable for eliminating strong background laser light and favors the detection of much weaker PL-emission from the nanowires.

Results and Discussion

Excitation of SPs in Composite ((Ag)SiO_2)CdSe Nanowires via CdSe NCs Emission. Illumination of plain metallic nanowires with a laser beam results in essentially two optical responses: (i) scattering of light at discontinuities of the nanostructure, e.g., tips and defects; (ii) coupling to SPs which propagate and decay both nonradiatively due to ohmic losses in the metal and radiatively with photon outcoupling at the same nanowire discontinuities. Experiments with plain silver nanowires[7] have demonstrated the possibility of direct plasmon excitation by evanescent fields of a prism (Kretschmann−Raether configuration), both with a spatially coherent laser source and broadband spatially incoherent light of a halogen lamp. Another way to excite SPs is to use nanoscale light emitters such as a molecules, luminescent nanoparticles, or the SNOM-tip in close vicinity of the metal surface.

The main goal of our experiment is to demonstrate the possibility of SP-excitation in the composite nanowire system via excitonic emission of the nanocrystals. The physical mechanism we explore here is based on the electromagnetic interaction of excitons with collective electron oscillations in silver nanowires and free-space photons. Energy released by

(21) Yin, Y.; Lu, Y.; Sun, Y.; Xia, Y. *Nano Lett.* **2002**, *2*, 427−430.

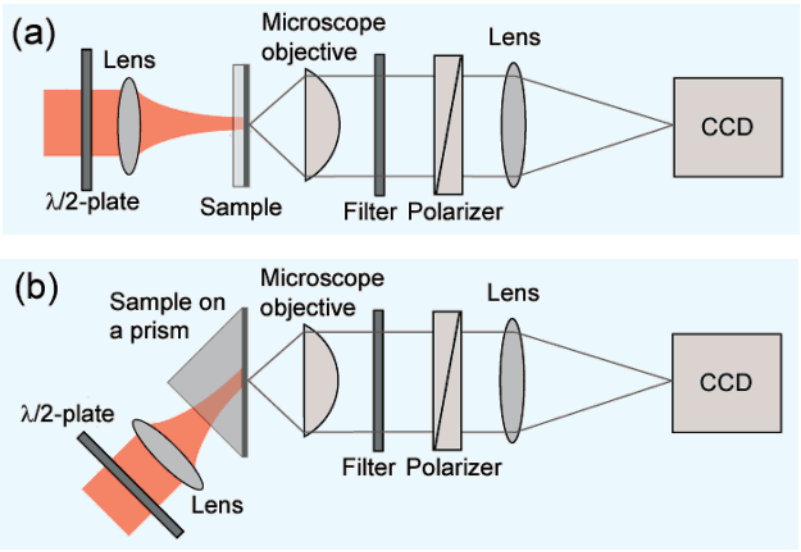

Figure 3. Micro-PL experimental setup. A frequency-doubled Nd:YAG laser ($\lambda = 532$ nm) is used as PL-excitation source. Two configurations were used to excite the samples: nanowires on a flat glass plate (a) or on a prism (b). Polarization of incident beam is controlled by rotating a half-wave plate and polarization of detection beam may be checked by rotating polarizer. The flat glass plate substrate is used for experiments with different polarizations of the incident laser beam. The polarization and intensity of the emission vs SiO_2 thickness were studied with prism configuration.

excitonic recombination in the nanocrystals (i) can be converted into and carried away by a propagating surface plasmon mode sustained by the metallic nanowire, (ii) can be converted into and carried away by free-space photon, or (iii) immediately dissipate into heat by metal electrons oscillated in the vicinity of the nanocrystal. The exciton−plasmon coupling is maximized by optimizing the distance between the nanocrystal and the nanowire surface. The excited surface plasmons start to propagate along the wire and couple to the electromagnetic field (i.e., emit free-space photons) at any discontinuity of the nanowire, especially at the nanowire tips. If the proposed simplified picture is appropriate to describe the investigated composite metal−insulator−semiconductor nanowire system, then it should demonstrate the following properties:

(i) Polarization dependence of the tip-enhanced emission should deviate from the polarization selection rules reported for laser excited plain metal wires (see ref 6 and 7);

(ii) A ratio between PL intensity measured at the tip and the middle of the nanowire should be larger than 1 and largest for the optimum spacer thickness *d*;

(iii) The spectrum of the tip emission should differ from uncoupled nanocrystal emission due to the spectral dependence of surface plasmons damping in the metal;

(iv) Nanocrystals with polarized emission, such as nanorods, should modify the exciton-plasmon interaction.

Figures 4−8 give a compilation of results from several independent measurements which evidence the exciton−plasmon interaction in composite ((Ag)SiO_2)CdSe nanowires.

First, in Figure 4 we compare PL-images of our composite ((Ag)SiO_2)CdSe nanowires in both excitation configurations on a glass plate and a prism (see Figure 3) for different polarization orientation in the incident laser (*I*) and emission detection (*E*) beams relatively to the nanowire axis. Figure 4 shows color-coded micro-PL images measured for a ((Ag)SiO_2)CdSe nanowire with 22 nm thick SiO_2 shell spectrally resolved at $\lambda = 605$ nm (the wavelength of CdSe QDs emission maximum) which is spectrally well-separated from the exciting laser wavelength ($\lambda = 532$ nm). The four images in Figure 4 correspond to four

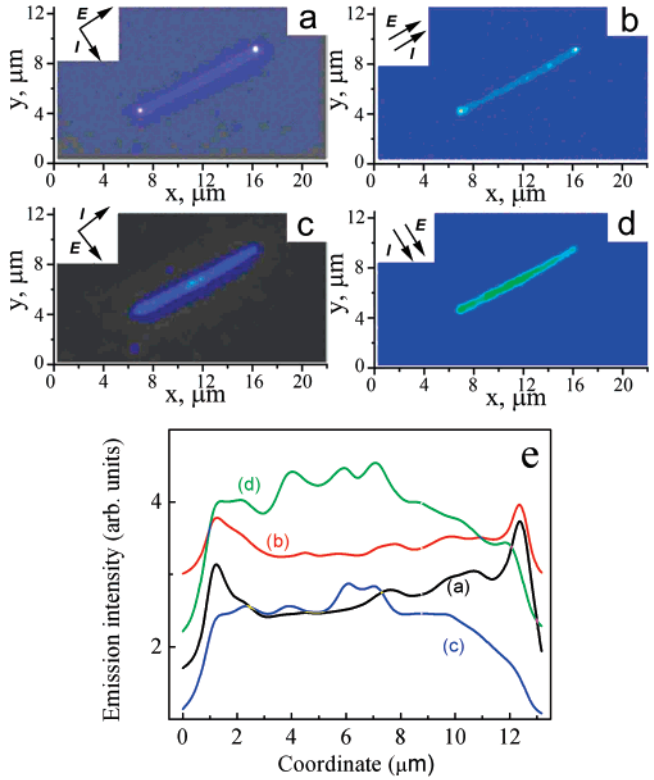

Figure 4. (a−d) Intensity-dependent false-color micro-PL images of a single composite ((Ag)SiO_2)CdSe nanowire ($d_{SiO_2} = 22$ nm) covered with CdSe QDs. Four different images relate to four different polarization orientations (with respect to the nanowire axis) of the incident (*I*) and the detection (*E*) beams. The emission intensity increases from black through blue to yellow. The polarizations direction is indicated by arrows on the corresponding images. (e) Emission intensity profiles recorded along the nanowire axis for images a−d measured directly with the CCD camera: the letters in brackets are related to corresponding images. $\lambda_{exc} = 532$ nm, $\lambda_{detection} = 605$ nm, $P_{exc} = 60$ mW. The sample was studied with the optical setup shown in Figure 3a.

different combinations in the polarization orientation of the *I* and *E* beam paths: $I_\perp$ and $E_\perp$ ($I_\parallel$ and $E_\parallel$) correspond to polarizations perpendicular (parallel) to the nanowire axis. From

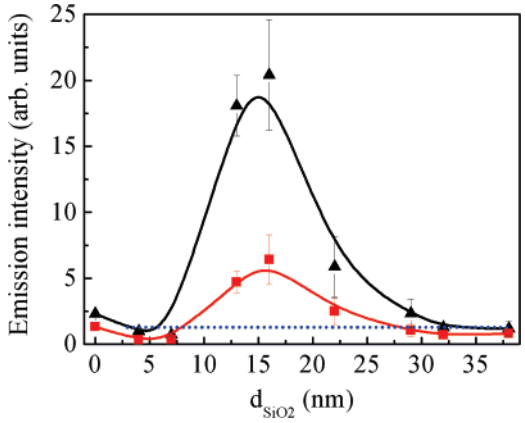

Figure 5. Emission intensity vs thickness of SiO_2 shell at the tip (black) and the middle (red) regions of a set of ((Ag)SiO_2)CdSe nanowires. The horizontal dotted blue line corresponds to the emission signal from hollow (SiO_2)QDs nanowire. $\lambda_{exc} = 532$ nm, $\lambda_{detection} = 605$ nm, $P_{exc} = 60$ mW.

the pairs of pictures (a, b) and (c, d), we conclude that the polarization orientation of *I* beam relative to the nanowire axis does not affect the spatial distribution of the emission intensity along the nanowire. In plain metallic wires, SPs can only be excited by the incident laser polarization possessing a component parallel to the nanowire axis, resulting to a strong polarization dependence of the tip emission. Therefore, we conclude that possible generation of SPs at the excitation wavelength by incident laser does not affect our measurements. Only the background signal is increased due to strong light scattering at the glass plate when the polarizations of both incident and emission beams are parallel to each other. Contrary to that, the micro-PL picture of a single nanowire changes drastically when the polarization orientation in the detection beam path changes from orthogonal ($E_\perp$) to parallel ($E_\parallel$) to the nanowire axis. In case of $E_\perp$, the nanowire emits light more or less homogeneously along the wire (Figure 4c,d), whereas the case of $E_\parallel$ reveals two bright spots at the nanowire tips (Figure 4a,b). This effect is clearly seen also in the emission intensity profiles along the nanowire axis plotted for different polarization orientations in Figure 4e. When we illuminate ((Ag)SiO_2)CdSe nanowire either with $I_\perp$ or $I_\parallel$, we homogeneously excite all QDs along the nanowire. The excitons in excited QD pass their energy to the nanowire SPs which propagate and scatter to free-space photons predominately at the nanowire discontinuities, i.e., tips. We conclude that the appearance of bright spots at both nanowire tips is a direct evidence for the efficient SP-excitation via CdSe NCs in our composite ((Ag)SiO_2)CdSe nanowires.

Next, we examined the dependence of the exciton−-plasmon interaction on the distance between the NCs and nanowire surface. Assuming the existence of a maximum in the emission intensity of the composite ((Ag)SiO_2)CdSe nanowires at a certain SiO_2 shell thickness, as observed earlier for colloidal gold films,[13] we performed a systematic study of the emission intensity for different SiO_2 shell thicknesses to find empirically the optimum Ag−NCs distance for the most efficient SP excitation. The result is shown in Figure 5. A set of composite ((Ag)SiO_2)CdSe nanowires was prepared with different SiO_2 shell thickness controlled by the amount of TEOS added during the shell growth. The exact SiO_2 shell thickness *d* was determined from the TEM images (Figure 1). Assuming the chemistry and thickness of the outer SiO_2 surface have no strong

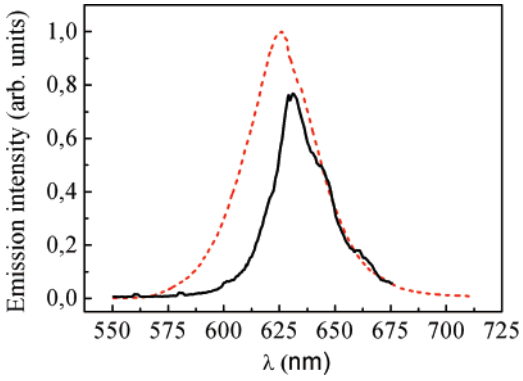

Figure 6. Micro-PL spectra of the tip emission from single ((Ag)SiO_2)-CdSe (black, solid) and single hollow (SiO_2)QDs nanowires (red, dashed). $\lambda_{exc} = 532$ nm, $P = 60$ mW.

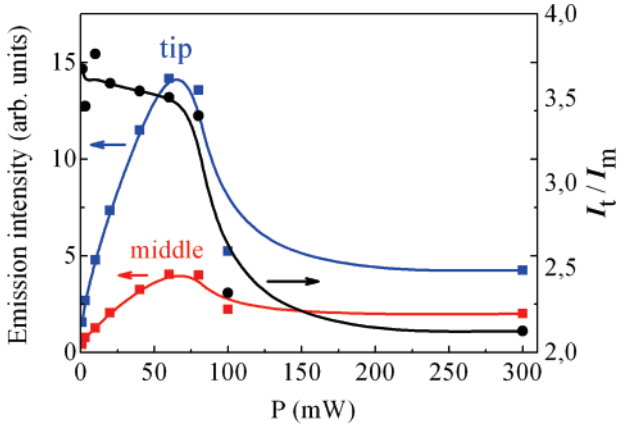

Figure 7. Pump power-dependent emission intensity at the tip (blue) and the middle (red) regions of ((Ag)SiO_2)CdSe nanowire and the ratio I_t/I_m for ((Ag)SiO_2)CdSe nanowire (black). I_t and I_m are the emission intensities at the tip and middle regions of nanowires, respectively. $\lambda_{exc} = 532$ nm, $\lambda_{detection} = 605$ nm.

influence on the NCs binding process, we obtained roughly equal surface density of QDs for all investigated ((Ag)SiO_2)-CdSe nanowires. The absolute value of the spectrally integrated emission has been measured at different points along the nanowire axis. Figure 5 shows the influence of SiO_2 shell thickness *d* on the emission intensity at the tips and middle region of a single ((Ag)SiO_2)CdSe nanowire. The optimum shell thickness $d = 15$ nm was found to yield the maximum in the emission intensity. At approximately $d > 35$ nm, the emission intensity approaches that for QDs without a metallic core beneath. The appearance of intensity maxima is in qualitative agreement with theoretical model by Ford and Weber who modeled the relaxation processes of optical emitters near metal surfaces and predicted the maximum of SP-emission rate for $d \approx 30$ nm.[22]

In Figure 5, we also compare the emission enhancement measured for the middle (I_m) and the tip (I_t) of the nanowire. For all distances *d* between 7 nm and 28 nm, the ratio of the intensities I_t/I_m is larger than 1, i.e., the absolute value of the emission intensity from the middle is smaller than that from the tips. This effect is attributed to weak outcoupling efficiency of SPs by surface roughness (I_m) as compared to the tips (I_t). Furthermore, we found an increase in I_t/I_m ratio up to a factor of 3.8 (see also Figure 7) for $7 < d < 15$ nm followed again by

(22) Ford, G. V.; Weber, W. H. *Phys. Rep.* **1984**, *113*, 195−287.

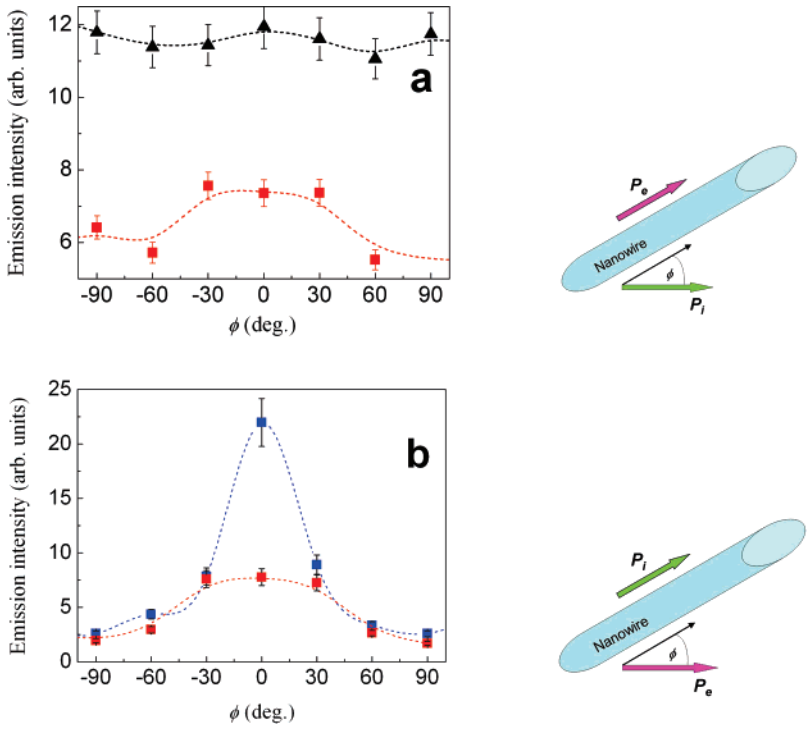

Figure 8. (a) Emission intensity from the middle region of single ((Ag)SiO_2)CdSe QDs (black) and ((Ag)SiO_2)CdSe NRs nanowires (red) vs polarization orientation of P_i beam toward the nanowire axis. Polarization orientation of P_e beam is fixed parallel to the nanowire axis. (b) Emission intenstity from the middle region of single hollow (SiO_2)CdSe NRs (blue) and ((Ag)SiO_2)CdSe NRs nanowires (red) vs polarization orientation of P_e beam toward the nanowire axis. Polarization orientation of P_i beam is fixed parallel to the nanowire axis. $d_{SiO_2} = 10$ nm, $\lambda_{exc} = 532$ nm, $\lambda_{em} = 605$ nm, $P = 60$ mW.

a decrease for larger d. The appearance of maxima both in the absolute intensity and the I_t/I_m ration at optimum shell thickness $d = 15$ nm confirms our assumption that the exciton−plasmon coupling is accompanied by SP propagation and a signal accumulation from many NCs.

Finally, from Figure 5 we can also derive an estimation for the efficiency of the exciton-plasmon coupling by comparing the emission intensity with that of the reference hollow (SiO_2)-CdSe nanowire. For a 15-nm thick SiO_2 shell the SP-mediated emission intensity from the tips of the ((Ag)SiO_2)CdSe nanowire is more than order of magnitude larger as compared to the reference hollow (SiO_2)CdSe nanowire.

Guiding of SPs in the Composite ((Ag)SiO_2)CdSe Nanowires. Because, the diameter of the excitation laser spot is greater than the nanowire length we excite the SPs via NCs emission along the whole nanowire length. The appearance of increased emission intensity from the nanowire tips we attribute to SPs propagation along the nanowire and scattering by the tips into free-space photons. In order to avoid artifacts, we performed a control experiment with hollow SiO_2 nanowires without Ag core ((SiO_2)CdSe nanowires). Such nanowires were produced by selective chemical etching of Ag core before attachment of CdSe NCs, as depicted in Figure 1. Hollow (SiO_2)CdSe nanowires show a nearly homogeneous emission signal along the whole length. The emission signal at the tips of the hollow (SiO_2)-CdSe nanowire drops smoothly, whereas for ((Ag)SiO_2)CdSe nanowire, it shows a sharp maximum. Further evidence for a waveguiding effect in a composite ((Ag)SiO_2)CdSe nanowire was obtained from comparison of room-temperature micro-PL spectra at the middle and the tips of both ((Ag)SiO_2)CdSe and hollow (SiO_2)CdSe nanowires (Figure 6). The emission maximum for ((Ag)SiO_2)CdSe nanowire is slightly shifted to longer wavelength as compared to hollow (SiO_2)CdSe nanowire, whereas the red parts of all spectra are almost co-incident. We believe that a small red shift of ((Ag)SiO_2)CdSe nanowire emission is caused by stronger SPs damping at shorter wavelength due to ohmic losses in the metal, a well-known property of SPs on metal-dielectric interfaces.

It is especially interesting to study the power dependent emission intensity from ((Ag)SiO_2)CdSe nanowires in order to get the information about possible nonlinear optical effects. Figure 7 shows power dependence of the emission intensity at the middle (I_m) and the tip (I_t) for single ((Ag)SiO_2)CdSe nanowire, as well as their ratio. The emission intensity grows almost linearly with increasing pump power P up to ~70 mW and decreases at higher values due to photochemical degradation of CdSe QDs. The ratio between I_t and I_m for ((Ag)SiO_2)CdSe nanowire is constant in the linear regime and (irreversibly) drops at higher power in agreement with suggested photochemical degradation of QDs.

Polarization Properties of SP Excited by CdSe NRs. Finally, we studied the polarization properties of both (Ag)-SiO_2 and hollow SiO_2 nanowires capped with CdSe NRs. Because, CdSe NRs absorb and emit strongly polarized light, it is of interest to examine the polarization sensitivity of the exciton−plasmon interaction. The general method for capping both hollow SiO_2 and (Ag)SiO_2 nanowires with CdSe NRs is the same, as for CdSe QDs and described above in the Experimental section. The micro-PL was measured for both single ((Ag)SiO_2)CdSe NRs and (SiO_2)CdSe NRs nanowires at room temperature and the intensity profiles along the nanowire axis were recorded as well as the polarization-dependence of the emission intensity at the tips and the middle of composite nanowires. A hollow (SiO_2)CdSe NRs nanowire as a reference sample was investigated also to identify the polarization properties of a NRs ensemble in the absence of plasmonic core.

We only discuss the angular dependence of emission intensity from the middle to avoid intrinsic polarizing effects of metal tips.

First, we have checked the dependence of the emission intensity from the middle of the composite ((Ag)SiO_2)CdSe NRs and ((Ag)SiO_2)CdSe QDs nanowires as a function of the polarization orientation P_i of the incident light (see Figure 8a). ((Ag)SiO_2)CdSe QDs nanowire shows a weak, less than 10%, deviation in the emission intensity with varied P_i, as expected for isotropic optical emitters. At the same time ((Ag)SiO_2)CdSe NRs sample shows pronounced maximum for P_i parallel to the nanowire axis with ~30% signal deviation. In order to understand this behavior in detail and investigate the role of SPs, we have compared the angular dependence of the emission from the middle of both ((Ag)SiO_2)CdSe NRs and hollow (SiO_2)CdSe NRs nanowires, shown in Figure 8b. It is clearly seen that in both cases, the emission possesses a maximum for P_e parallel to the nanowire axis with much stronger effect in the reference (SiO_2)CdSe NRs nanowire. Since, we do not expect any influence of hollow SiO_2 nanowire on polarization properties of CdSe NRs, the observed strong angular dependence of emission along the nanowire axis indicates on a preferential unidirectional orientation of CdSe NRs along the nanowire axis.

Earlier, we calculated and verified experimentally that for the two-dimensional ensemble of randomly oriented CdSe NRs on a flat glass surface at room temperature the ratio $R = E^{\perp}/E^{\parallel}$ (where $E^{\perp}$ and $E^{\parallel}$ are the emission intensities for P_e perpendicular or parallel to P_i) cannot be smaller than $R \approx 0.7$ (0.75 for three-dimensional ensemble of randomly oriented nanorods in polymeric matrices).[23] Simultaneously, for single CdSe NRs we found $R \approx 0.1$. The value of R derived from Figure 8b is about 0.12, which represents strong evidence for alignment of CdSe NRs on the surface of the SiO_2 shell. Here, a relatively small diameter of nanowires provokes CdSe NRs to orient preferentially along the nanowire axes. Hence, we may expect that the spatial organization of CdSe NRs on the surface of the nanowire is similar to that of hollow (SiO_2)CdSe NRs nanowire. We explain a much weaker angular dependence of the ((Ag)-SiO_2)CdSe NRs emission by efficient excitation of SPs by CdSe NRs. Indeed, our interpretation assumes that PL emission from the middle of the nanowires is governed by outcoupling of SPs by surface roughness. The expected strong depolarization by surface roughness of SPs scattered into free-space photons is likely to suppress the strong intrinsic anisotropy in the emission from the aligned CdSe NRs.

(23) Artemyev, M.; Möller, B.; Woggon, U. *Nano Lett.* **2003**, *4*, 509−512.

Conclusions

We presented a simple and reproducible synthesis of composite metal−insulator−semiconductor nanowires ((Ag)SiO_2)-CdSe nanowires) of desired diameter and length. Silver nanowires are covered with a SiO_2 shell of controlled thickness which preserves the silver core from chemical destruction (oxidation, sulfidization etc.) and adjusts the optimal distance between nanoscale light emitters (here, CdSe quantum dots and nanorods) and metal surface to increase the efficiency of the exciton−plasmon interaction. By a detailed analysis of the polarization dependence of the nanowire emission and its intensity distribution along the nanowire axis, the plasmon-assisted nature of the nanowire emission has been proven. The improvement of the procedure for quantum dots deposition, mainly the increase of their surface concentration or multilayer NCs deposition represents a challenge that might allow nonlinear optical phenomena in the exciton-plasmon interactions to be observed.

Acknowledgment. M.A. and E.U. gratefully acknowledge the programs CHEMICAL REAGENTS AND MATERIALS and KRYSTALLINE & MOLECULAR STRUCTURES (project 40.3). Financial support by the DFG (Graduiertenkolleg GRK 726, Wo477/23,25) and the NoE PHOREMOST are gratefully acknowledged.

JA074705D